BALLISTIC PENETRATION AND PERFORATION OF LAYERED STEEL PLATES: AN EXPERIMENTAL AND NUMERICAL INVESTIGATION

S. Dey[1,2] and T. Børvik[1,2]

[1] *Norwegian Defence Estates Agency, Research & Development Department, PB 405, Sentrum, NO-0103 Oslo, Norway. e-mail: sumita.dey@forsvarsbygg.no*

[2] *Structural Impact Laboratory (SIMLab), Department of Structural Engineering, NTNU, NO-7491, Trondheim, Norway. E-mail: sumita.dey@ntnu.noTT*

In the design of protective structures, thin plates of high-strength steel are frequently being used both in civil and military ballistic protection systems. Earlier studies have shown that by changing the target thickness the deformation mode changes accordingly, from thin plate global deformation towards thick plate shear localisation. Thus, the global deformation mode in thin plates may absorb considerable amount of energy, and it can be presumed that layered targets may be a better energy absorber during ballistic perforation than a monolithic target of equal thickness. Some publications in the literature indicate that this is not necessarily true, but the data on impact of layered targets is limited and it is difficult to make comparisons between results. At present the effect of replacing monolithic plates with layered ones is not clear and further work is required.

In this study, the response to normal impact of hardened ogival steel projectiles on layered steel plates has been investigated both experimentally and numerically. In the tests, 12 mm thick (monolithic or layered) plates of Weldox 700 E were impacted using a gas-gun at sub-ordnance velocities and the ballistic limit of the different target combinations were obtained. Numerical simulations of the perforation processes were carried out using LS-DYNA. Both qualitatively and quantitatively good agreements were found between experimental and numerical results.

INTRODUCTION

The idea of using layered plates instead of a monolithic one of equal weight in order to increase the ballistic perforation resistance is not new, and the effect of using targets made up of several thinner plates has been investigated in the literature for a long time. An overview of some of the studies can be found in Dey et al. [1]. From this,

it may be concluded that the data on impact of multi-layered targets is limited and it is difficult to make comparisons between experimental results. Hence, at present the effect of replacing monolithic plates with multi-layered ones is therefore not clear and further experimental and numerical work is needed.

In a recent study by Teng et al. [2], the protection performance of double-layered metal shields against projectile impact was studied in a pure numerical approach using ABAQUS/Explicit. Four types of projectiles at different weight and nose shape were considered, representing various fragments generated from improved explosive devises (IEDs). These numerical simulations revealed the possible advantageous by using a double-layered target instead of a monolithic one of equal weight in ballistic protection. In an extensive study by Dey et al. [1], the ballistic perforation resistance of double-layered steel plates impacted by blunt and ogival projectiles were investigated both experimentally and numerically (with LS-DYNA). In the tests, 12 mm thick (monolithic or layered) targets of Weldox 700 E were impacted using a compressed gas-gun at sub-ordnance velocity and the ballistic limit of the various target combinations was obtained. In general, good agreement was obtained between numerical simulations and experimental results, and the main conclusion was that the overall protection level seems to increase significantly by layering the target. In the present paper some of the main findings using ogival projectiles from the study by Dey et al. [1] will be presented. It is referred to Dey et al. [1] for more detailed discussion and conclusion on both blunt and ogival projectiles.

EXPERIMENTAL WORK

Test Set-Up

The target plates were made of Weldox 700 E steel, which is a tempered martensittic steel that has both high strength as well as relatively high ductility. Results obtained from a standard quasi-static tensile test on a smooth axisymmetric specimen at room temperature show a yield stress of above 850 MPa and a failure strain as high as 1.2 at a true stress of about 1550 MPa. Details from an extensive material characterization of this steel alloy can be found in Dey et al. [3].

The ballistic perforation resistance of a 12 mm thick monolithic Weldox 700 E plate has previously been obtained using ogival projectiles [3]. In the following, this test result will be compared with two new target configurations of equal thickness, material and weight using double-layered plates. The new configurations consist of two 6 mm plates in full contact (i.e. 2x6 mm) and two 6 mm plates spaced with 24 mm air (i.e. 2x6 + 24 mm). The projectiles were ogival nosed and made of hardened tool steel with a nominal mass, diameter and hardness of 197 g, 20 mm and HRC 52 ($\sigma_0 \sim 1900$ MPa), respectively. The geometry of the projectile can be found in Dey et al. [1].

The ballistic tests were carried out in the compressed gas gun at SIMLab described by Børvik et al. [4]. The steel projectiles were mounted in a nine-pieced sabot and launched at impact velocities just below and well above the ballistic limit velocity, i.e. the critical impact velocity of the target configuration. The sabot pieces were stopped by a sabot trap prior to impact. The targets were clamped in a circular frame by 16 prestressed bolts, having a free span diameter of 500 mm in all tests. The penetration event was captured by a Photron Ultima APX-RS digital high-speed video camera operating at a constant framing rate of 50.000 fps. Initial and final velocities were measured using different laser-based optical devices, as well as by the high-speed camera system. Both initial and final target deformations were measured in-situ before and after each test. Details regarding the test set-up and instrumentation used during testing can be found in Børvik et al. [4].

Test Results

By keeping all parameters constant except for the impact velocity of the projectile, the ballistic limit velocity of the various target configurations could be determined. The ballistic limit was calculated as the average between the highest impact velocity not giving perforation and the lowest impact velocity giving complete perforation of the target. Knowing the ballistic limit velocity from the experimental tests, curves through the data points were fitted to an analytical model originally proposed by Recht and Ipson [5]

$$v_r = a(v_i^p - v_{bl}^p) \tag{1}$$

The model is based on the conservation laws, so in the original model $a = m_p/(m_p+m_{pl})$, where m_p and m_{pl} are the mass of the projectile and plug, respectively, $p = 2$ and v_{bl} is the ballistic limit velocity. As ogival projectiles induce failure by ductile hole growth without plugging, the parameter a will be equal to 1 for ogival projectiles. Hence, only p was fitted to the experimental results using the method of least squares, since the ballistic limit velocity was always taken directly from the experimental data. The experimental data with fitted curves can be seen in Figure 1, while the values of a, p and v_{bl} can be found in Dey et al. [1]. As seen, the monolithic target protects better than the double-layered target for ogival projectiles, but the difference in perforation resistance is only about 10-15 %. Further, it is seen that there is hardly any difference in ballistic limit velocity between the double-layered targets when the plates are in contact or spaced with 24 mm of air. Additionally, Figure 1 shows one test result using a target configuration with only 12 mm air gap struck by an ogival projectile. From this result it seems that the size of the air gap does not influence the ballistic resistance as long as the spacing is moderate. That targets impacted by ogival projectiles fail by ductile hole growth are clearly seen from the high-speed camera images of the perforation process in

Figure 2. In this failure mode the material is pushed aside by the moving projectile due to plastic flow around the nose tip.

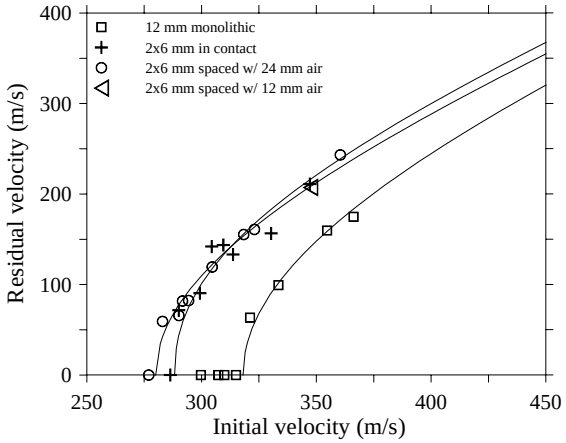

Figure 1. Residual versus initial velocities for three different target configurations with total thickness of 12 mm impacted by ogival projectiles.

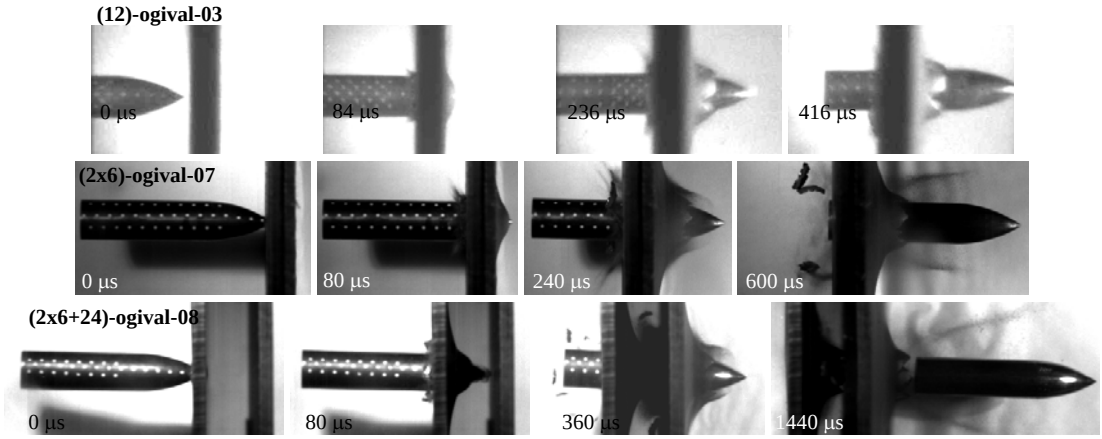

Figure 2. Images of the perforation process for the three target configurations at impact velocities close to their respective ballistic limits.

NUMERICAL SIMULATIONS

Numerical Set-Up

The impact tests were analysed using the explicit solver of the non-linear finite element code LS-DYNA [6]. The target was modelled using slightly modified versions of the well-known Johnson-Cook constitutive relation and fracture criterion. The equivalent stress in the constitutive relation is expressed as [7, 8]

$$\sigma_{eq} = (A + B\varepsilon_{eq}^{n})(1 + \dot{\varepsilon}_{eq}^{*})^{C}(1 - T^{*m}) \tag{2}$$

where A, B, n, C and m are material constants determined from material tests, the dimensionless strain rate is given as $\dot{\varepsilon}_{eq}^{*} = \dot{\varepsilon}_{eq} / \dot{\varepsilon}_{0}$ and the homologous temperature is given as $T^{*} = (T - T_r)/(T_m - T_r)$. Here, $\dot{\varepsilon}_{0}$ is a user-defined strain rate and the suffixes r and m indicate room and melting temperature, respectively. The fracture strain in the fracture criterion is given as [7, 9]

$$\varepsilon_f = (D_1 + D_2 \exp(D_3\sigma^{*}))(1 + \dot{\varepsilon}_{eq}^{*})^{D_4}(1 + D_5 T^{*}) \tag{3}$$

where D_1,…D_5 are material constants determined from material tests, and $\sigma^{*} = \sigma_H / \sigma_{eq}$ is the stress triaxiality ratio. Fracture occurs when damage of a material element equals unity, since no coupling between the damage and the constitutive relation is considered in this study. The damage D is expressed as

$$D = \sum \frac{\Delta\varepsilon_{eq}}{\varepsilon_f} \leq D_C = 1 \tag{4}$$

where $\Delta\varepsilon_{eq}$ is the increment of the accumulated (equivalent) plastic strain. When the damage in an element reaches its critical value (D_c = 1), the element fails by element erosion (i.e. the stresses in the integration point are set to zero). These two models have previously been found to give good results in similar studies by the authors. As the constitutive models are used for adiabatic conditions, the temperature increase due to adiabatic heating was calculated as [10]

$$\Delta T = \int_0^{\varepsilon_{eq}} \chi \frac{\sigma_{eq} d\varepsilon_{eq}}{\rho C_p} \tag{5}$$

where ρ is the material density, C_p is the specific heat, and χ is the Taylor-Quinney coefficient that gives the proportion of plastic work converted into heat. The projectile of hardened tool steel was modelled as a bilinear elastic-plastic von-Mises material with isotropic hardening without fracture using Material Type 3 in LS-DYNA. The material constants for both the Weldox 700 E targets and the projectile are given in Dey et al. [1], where also further details about the numerical model can be found.

The geometry of the targets and projectiles was identical to that used in the experimental tests. As in the experimental tests, targets were modelled as circular symmetric with a free-span diameter of 500 mm and fully clamped at the support, while the projectiles had a nominal mass and diameter of 197 g and 20 mm, respectively. The mesh consisted of 4-node axisymmetric 2D elements with one integration point and stiffness-based hourglass control. Contact between the projectile and target was

modelled using an automatic 2D single surface penalty formulation without friction [6]. As the failure mode is ductile hole growth, adaptive updating was necessary using the re-meshing algorithm available in LS-DYNA. The initial element size in each plate was chosen equal to 0.3 x 0.3 m^2, giving 40 elements over the target thickness. The ogival projectile had a much coarser mesh than the target, with an initial element size varying from 1.0 x 3.0 mm^2 to 1.0 x 0.1 mm^2 towards the pointed nose.

In all simulations the projectile was given an initial velocity identical to the one used in the corresponding experiment, and the residual velocity of the projectile was registered. From this, the ballistic limit velcoty was estimated based on 7-8 simulations and the Recht-Ipson model given in eq. (1). Here, the model constants p and v_{bl} were fitted to the numerical results using the method of least square, while a was kept equal to 1.

Numerical results

The numerical results are shown in Figure 3. As seen, the trend obtained experimentally are correctly captured in the numerical simulations, and the ballistic perforation resistance is found to be lower for a double-layered target than for a monolithic target. It has also been studied numerically whether the size of the air gap between the two plates have any influence on the ballistic limit velocity. Experimentally one test indicated that a reduction in spacing from 24 mm to 12 mm was not important as long as the plates do not intersect with each other (see Figure 1). Numerically the air gap was varied from 12 mm to 72 mm, and it was found that the size of the air gap does not influence the ballistic limit velocity or the residual velocity of the projectile. This is as expected (as long as pitch, yaw and tumbling is prevented) and in agreement with the experimental observation.

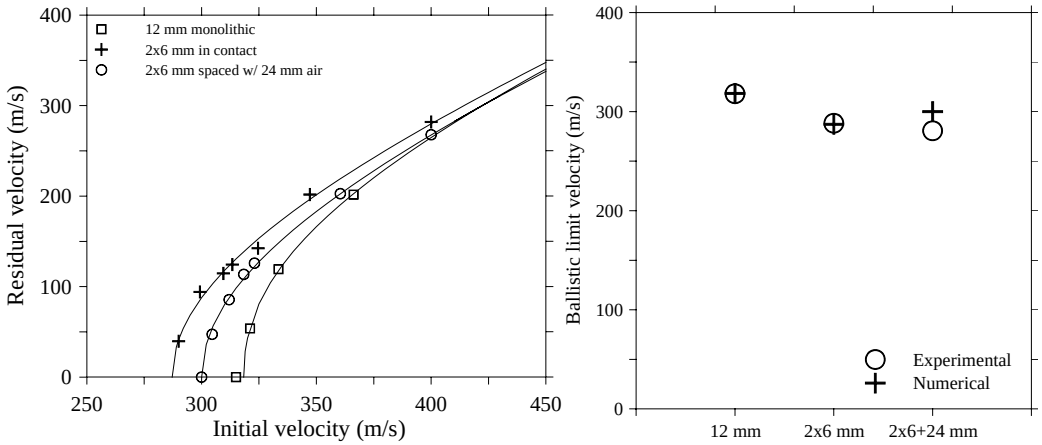

Figure 3. Numerically obtained residual versus initial velocity curves for the three different target configurations (left), and comparison between experimental and numerical ballistic limits (right).

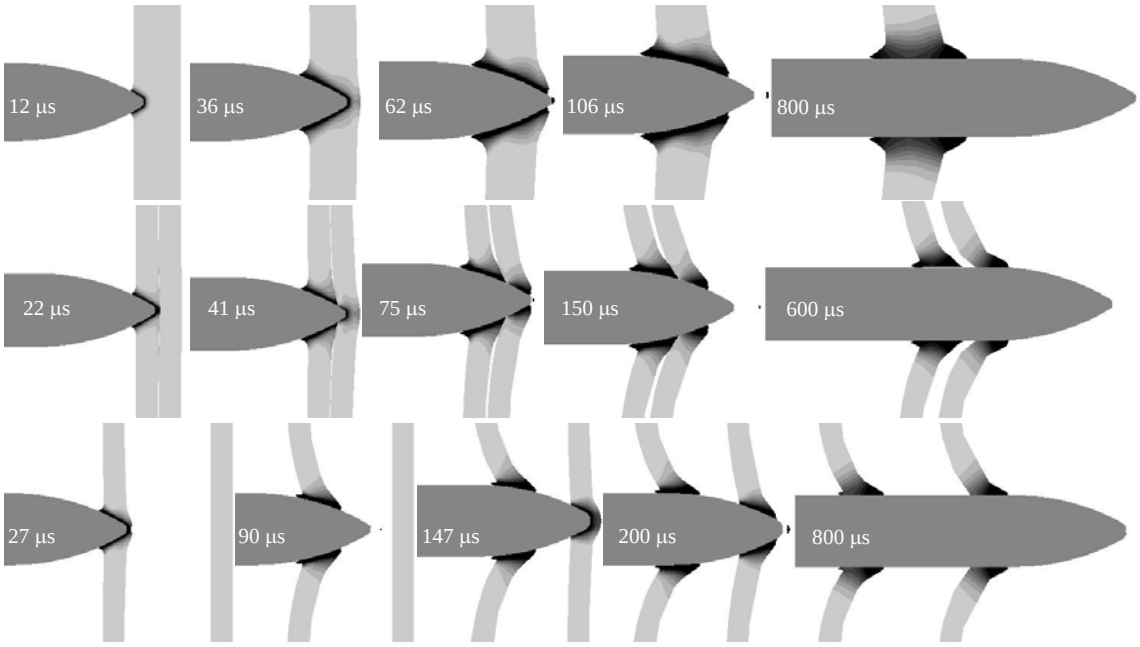

Figure 4. Plots of the perforation process for the three target configurations. The impact velocities are close to their respective ballistic limit velocity. The targets are plotted as fringes of effective plastic strain in the user-defined range from $\varepsilon_{eq} = 0$ (light grey) to $\varepsilon_{eq} = 1$ (black).

Figure 3 also compares numerical predictions of the ballistic limit velocities to the experimental results. As seen, the numerical predictions are close to the experimental results. Figure 4 shows plots of the perforation process for the three different target configurations. The targets are plotted with fringes of effective plastic strain, where the maximum plastic strains in the black area is equal to or higher than 1. It is seen that the plastic strain accumulates around the projectile nose as expected for this failure mode. Note that the minor petals observed in the experimental tests (see Figure 2) can not be predicted using 2D axisymmetric elements, and due to adaptive re-meshing, the rear side of the plates in some of the simulations became somewhat jagged. However, it is not believed that this have any effect on the obtained numerical predictions of the ballistic limit velocity.

CONCLUDING REMARKS

By double-layering a 12 mm thick target impacted by ogival projectiles, a decrease in ballistic limit velocity of about 10 % is obtained both for plates in contact and plates spaced with 24 mm of air compared to a monolithic target. Further, both qualitative and quantitative good agreements are obtained between the numerical simulation and experiment results. Thus, it may be concluded that non-linear finite

element simulations are able to capture the main physical behaviour during perforation of both monolithic and double-layered steel plates, at least within the limitations of this study.

REFERENCES

[1] S. Dey, T. Børvik, X. Teng, T. Wierzbicki, O.S. Hopperstad, On the ballistic resistance of double-layered steel plates: An experimental and numerical investigation, *Submitted for possible journal publication*, (2006)
[2] X. Teng, S. Dey, T. Børvik, T. Wierzbicki, Protection performance of double-layered metal shields against projectile impact, *Submitted for possible journal publication*, (2006)
[3] S. Dey, T. Børvik, O.S. Hopperstad, J.R. Leinum, M. Langseth, The effect of target strength on the perforation of steel plates using three different projectile nose shapes, *International Journal of Impact Engineering*, **30**, 1005-1038 (2004)
[4] T. Børvik, O.S. Hopperstad, M. Langseth, K.A. Malo, Effect of target thickness in blunt projectile penetration of Weldox 460 E steel plates, *International Journal of Impact Engineering*, **28**, 413-464 (2003)
[5] R.F. Recht, T.W. Ipson, Ballistic perforation dynamics, *Journal of Applied Mechanics*, 384-390 (1963)
[6] J.O. Hallquist, Keyword User's Manual, Version 970. Livermore Software Technology Corporation, California. (2003)
[7] T. Børvik, O.S. Hopperstad, T. Berstad, M. Langseth, A computational model of viscoplasticity and ductile damage for impact and penetration, *European Journal of Mechanics, A/Solids*, **20**, 685-712 (2001)
[8] G.R. Johnson, W.H. Cook, A constitutive model and data for metals subjected to large strains, high strain rates and high temperatures, *Proceedings of the 7th International Symposium on Ballistics*, 541-547 (1983)
[9] G.R. Johnson, W.H. Cook, Fracture characteristics of three metals subjected to various strains, strain rates, temperatures and pressures, *Engineering Fracture Mechanics*, **21**, 31-48 (1985)
[10] J. Lemaitre, J.-L. Chaboche, Mechanics of Solid Materials. Cambridge University Press, Cambridge. (1990)